Elastic Behavior of Normally Consolidated Clay

S. OHMAKI
National Research Institute of Fisheries Engineering, Hiratsuka, Japan

1 INTRODUCTION

In general, soil exhibits an irreversible stress-strain behavior and a hysteresis loop in the loading-unloading-reloading process. Such characteristics are shown in both volumetric and shearing strains. Therefore, in order to take such phenomenon into account when formulating the stress-strain relationship, it is neccesary to study the behavior of soil after yielding, as well as during the yielding process.

Some investigators have pointed out that there might be two modes of soil yielding, i.e., volumetric change and shearing deformation. They have suggested that these characteristics should be taken into account in formulating a stress-strain relationship (Poorooshasb, 1966, Tatsuoka and Ishihara, 1974, Nishi and Esashi, 1978, Vermeer, 1978, Ohmaki, 1979).

Accordingly, it is assumed in this paper that elastic as well as plastic strains can each be divided into two components one of which is caused by changes in the stress ratio and the other by changes in the mean effective stress. In order to clarify the properties of these two components of elastic strain, two kinds of loading-unloading-reloading tests were carried out. One was a cyclic test of stress ratio, in which the mean effective stress was kept constant and the other was a cyclic test for mean effective stress, in which the stress ratio was kept constant. Results of experiments in which the stress ratio was decreased and the mean effective stress was increased simultaneously are also shown. Based upon these experimental results, a simple, empirical law for stress-strain behavior under axisymmetric conditions is proposed.

2 PROCEDURE USED TO ANALYZE EXPERIMENTAL RESULTS

Results of drained shear tests on clay, performed under triaxial compression and extension conditions, are examined here. In the analysis, the following parameters are used:

$$p = \frac{1}{3}(\sigma_a' + 2\sigma_r'),\ q_a = \sigma_a' - \sigma_r',\ \eta_a = \frac{q_a}{p},$$

$$v = \varepsilon_{axial} + 2\varepsilon_{rad},\ \varepsilon_a = \frac{2}{3}(\varepsilon_{axial} - \varepsilon_{rad}),$$

where, σ_a' and σ_r' denote axial and radial effective principal stresses, and ε_{axial} and ε_{rad} denote strains in axial and radial directions, respectively, of the cylindrical specimen.

Now, we express the increments, dv , of volumetric strain and $d\varepsilon_a$ of deviatoric strain as follows:

$$dv = dv^e + dv^p = dv^e_\eta + dv^e_p + dv^p_\eta + dv^p_p , \quad (1)$$

$$d\varepsilon_a = (d\varepsilon_a)^e + (d\varepsilon_a)^p$$
$$= (d\varepsilon_a)^e_\eta + (d\varepsilon_a)^e_p + (d\varepsilon_a)^p_\eta + (d\varepsilon_a)^p_p , \quad (2)$$

where superscripts e and p denote elastic and plastic components, respectively. Strain increments with subscripts η and p will be called the η-component and p-component of the strain. Experimentally, we obtain the η-component of the volumetric and deviatoric strain increments from triaxial tests in which the stress ratio is increased or decreased while p is kept constant. The p-component of these increments is obtained from tests in which mean effective stress is increased or decreased while the stress ratio is kept constant. In tests where p and η_a change simultaneously, the strain increment obtained is the sum of each component, as expressed in eqs. (1) and (2).

In this paper, we consider only results of experiments in which the stress ratio $|\eta_a|$ is decreased. Thus the η-components of plastic strain increments, dv^p_η and $d\varepsilon^p_\eta$, in equations (1) and (2) drop out and these equations can be rewritten as follows:

$$dv = dv^e_\eta + dv^e_p + dv^p_p \quad (3)$$

$$d\varepsilon_a = (d\varepsilon_a)^e_\eta + (d\varepsilon_a)^e_p + (d\varepsilon_a)^p_p \quad (4)$$

When (-de) is used to denote a decrement of the void ratio, the following relationship is obtained:

$$(-de) = (1 + e)\, dv \quad (5)$$

3 SAMPLES AND TEST PROCEDURES

The gray silty clay which was used in this study was taken from Fujinomori, in the southern part of Kyoto Prefecture, Japan. Its liquid limit is 43.6 % and plastic limit 26.1 %. The texture of this soil is as follows: clay 17.5 %, silt 50.8 % and sand 31.7 %. The specific gravity is 2.648. The sample used in the experiment was remoulded and reconsolidated. Details of the sample preparation are described in another paper (Ohmaki, 1979). Samples were trimmed to cylindrical specimens 35 mm in diameter and 79 mm in height. They were placed in a triaxial cell and covered with rubber membranes. For consolidation and shearing, samples were placed on a pedestal and converted to porous stone by draining through filter paper. Frictionless end platens were used which were covered with rubber membranes, lubricated with silicone grease. During the tests, the volume of water expelled from the specimen was measured with a burette and the displacement at the top of the

specimen was measured with a dial gauge, through the loading piston. All the tests were performed under controlled stress conditions in a temperature controlled room set at 20 ± 0.5 °C.

4 EXPERIMENTAL RESULTS

4.1 Results of constant p tests

Figure 1 shows results of the loading-unloading-reloading tests for stress ratio, η_a, performed under triaxial compression and extension, with p held constant (= 2 kgf/cm^2). The relationship between η_a and ε_a is shown in Figure 1(a). It is evident in this figure that the hysteresis loop is small if the amplitude of the shear stress ratio is small. Figure 1(b) shows the relationship between volumetric strain, v, and stress ratio, η_a. In this figure it can be seen that, when the amplitude of η_a is small, the specimen always contracts in both unloading and reloading under triaxial compression and extension. On the other hand, where the amplitude of η_a is large, the soil specimen tends to dilate.

Next, results of simple unloading tests for η_a with p kept constant are shown. The stress paths used are shown in Figure 2. Soil specimen were consolidated isotropically by increasing the value of p in steps, 0.5, 1.0, 2.0 and 4.0 kgf/cm^2, at two day intervals. Then, after the specimen was sheared to the stress ratio η_{ai} with p kept constant, the shear stress was reduced step by step, as shown in Figure 2. The

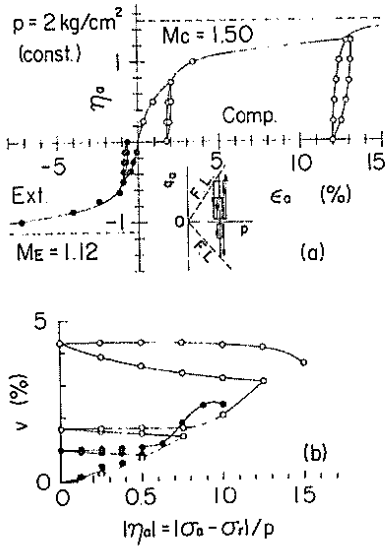

Figure 1 Cyclic shear test results with p kept constant

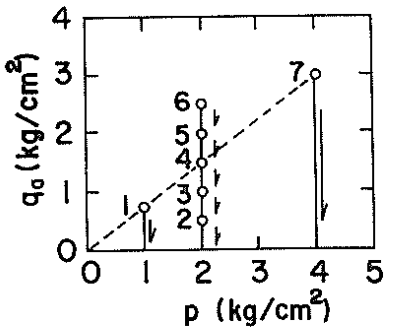

Figure 2 Stress paths of unloading tests with p kept constant

specimen was both loaded and unloaded in steps, separated by one day intervals. These steps are indicated by plots in Figures 3 and 4. For tests where p equals 2 kgf/cm^2, 0.25, 0.50, 0.75, 1.00 and 1.25 were taken as values of η_{ai}. However, for tests where p equals 1.0 and 4.0 kgf/cm^2, a η_{ai} value of 0.75 was used. Test results are shown in Figure 3. It is apparent in Figure 3(a) that $\eta_a \sim \varepsilon_a$ curves are parallel to each other irrespective of η_{ai}. It is also apparent in Figures 3(b) and (c) that $v \sim \eta_a$ curves as well as $(-\delta e) \sim \eta_a$ curves are parallel irrespective of η_{ai}. Figure 4 shows the results of unloading tests for η_{ai} equal to 0.75 with p kept constant (= 1.0, 2.0 and 4.0 kgf/cm^2). In Figure 4(a) the $\eta_a \sim \varepsilon_a$ curves are parallel to each other during unloading, although during loading they are fairly different, depending on the value of p. In Figure 4(b) the $\eta_a \sim v$ curves are also parallel to each other during unloading.

Now, we have seen from the unloading and reloading tests under constant p, that $\eta_a \sim \varepsilon_a$ curves under this condition are parallel to each other and that $\eta_a \sim v$ curves are independent of p. These properties are idealized in Figure 5. That is, we assume that the relationship between normalized stress ratio $|\eta_a/M|$ and $|\varepsilon_a|$ during unloading and reloading under constant p, where M is the stress ratio $|\eta_a|$ at failure, can be expressed as a straight line with a slope of G. Another idealized relationship is shown in Figure 5(b), in which it is likewise assumed that the relationship between v and $|\eta_a/M|$ can be expressed as a straight line with a slope of ± d and that the specimen always contracts under the conditions described above.

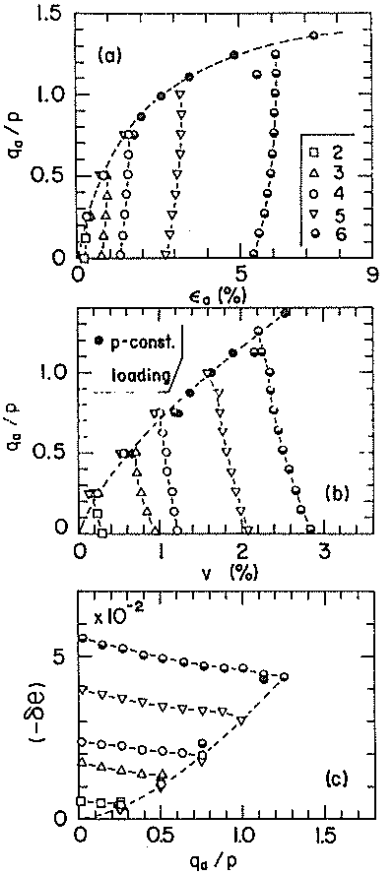

Figure 3 Unloading test results with p kept constant (p = 2 kgf/cm^2)

As a results of these assumptions, strain increments under the above conditions are expressed as follows.

$$dv^e_\eta = \frac{d}{M} |d\eta_a| \quad (6)$$

$$(d\varepsilon_a)^e_\eta = \frac{G}{M} d\eta_a \quad (7)$$

It is reasonable in these equations that M take the value corresponding to triaxial compression or extension. An expression similar to equation (6) is used by Karube and Kurihara (1966).

4.2 Results of the constant η_a tests

Next we show the results of tests in which mean effective principal stress was loaded, unloaded and reloaded while keeping the stress ratio constant (constant η_a). Figure 6 shows the stress paths used in these tests. Tests were carried out as follows: After the specimens were consolidated isotropically at p equal to 0.5 kgf/cm^2 for one day, they were sheared under triaxial compression and extension to the stress ratio η_{ai}, while p was kept constant. Then, p, the mean effective stress, was increased, decreased and again increased, while η_a was kept constant (= η_{ai}). This was done in steps, indicated in Figure 6, separated by one day intervals.

In Figure 7, (-δe) ∿ log p data from these tests are plotted. For these tests the (-δe) ∿ log p curves for swelling and recompression are parallel to each other and independent of η_{ai}. Therefore we can say

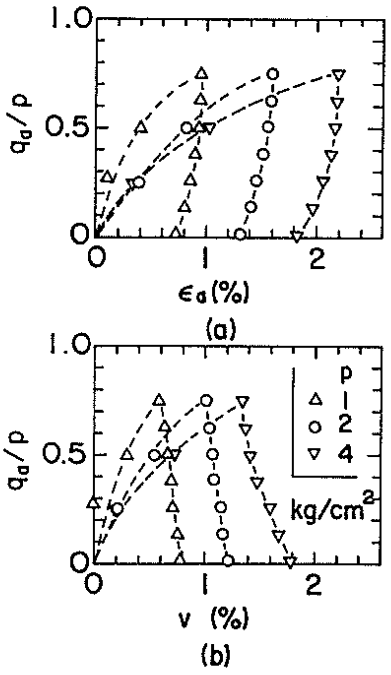

Figure 4 Unloading test results with p kept constant (η_{ai} = 0.75)

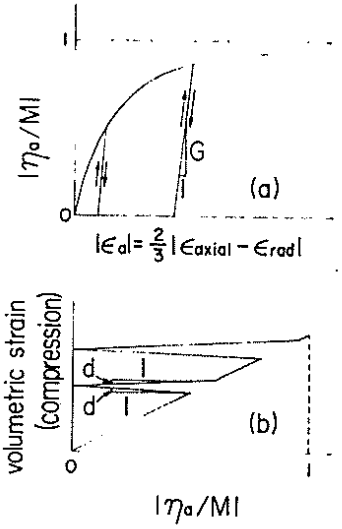

Figure 5 A stress-strain model of soil during shear with p kept constant

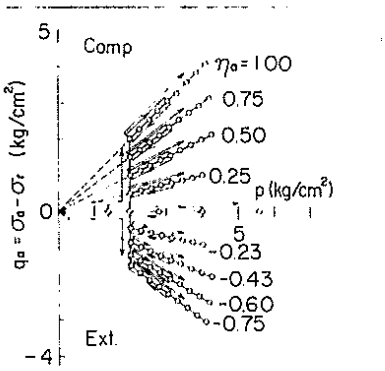

Figure 6 Stress paths of cyclic tests of p

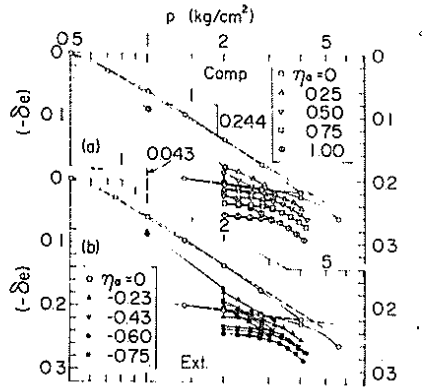

Figure 7 e ∿ log p plots of cyclic tests of p

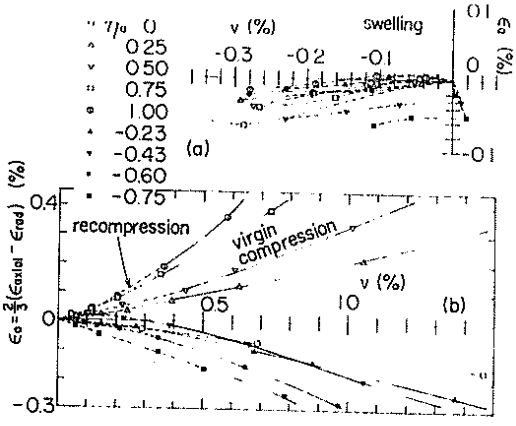

Figure 8 ε_a ∿ v relations during (a) swelling, (b) recompression with stress ratio kept constant

that the slope of these curves is equal to the swelling index, Cs (= 0.043), of the isotropic swelling test. Here we take 0.244 as the value of the compression index, Cc , from the virgin consolidation curve in this figure. The relationships between ε_a and v during the swelling and recompression parts of these tests are shown in Figure 8 (a) and (b), respectively. It is apparent in Figure 8(a) that ε_a is negligibly small compared with v , and it tends to decrease slightly as v decreases. Since this tendency appeared in the test performed under isotropic stress conditions, it is considered to be due to anisotropy inherent in the specimen. Figure 8(b) shows relationships between ε_a and v during recompression. Dashed portions of curves denote regions of overconsolidaton and solid portions denote normal consolidation. It can be seen in this figure that slopes of $\varepsilon_a \sim v$ curves increase gradually as η_{ai} increases and that curves are convex towards the v-axis. That is,

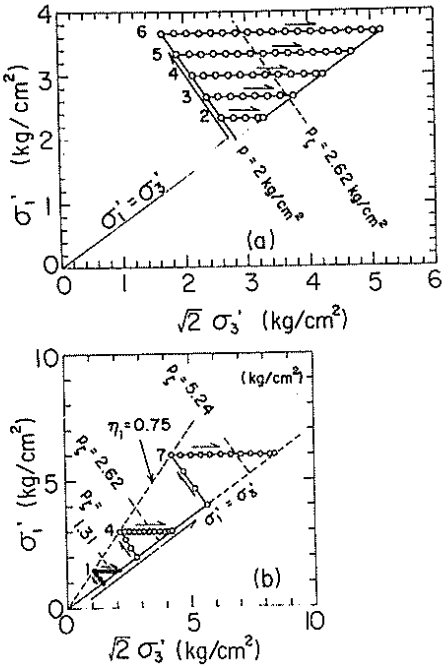

Figure 9 Stress paths of the unloading tests with σ_a' kept constant

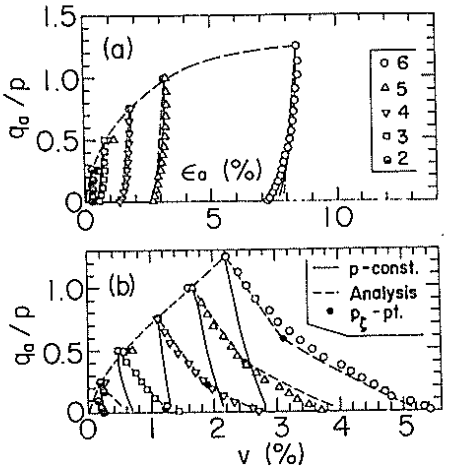

Figure 10 Comparison between experimental and analytical results of constant σ_a' tests. (p = 2 kgf/cm²)

deformation of the specimen is not isotropic. Using the results of the swelling tests, we can express the strain increments, dv_p^e , and $(d\varepsilon_a)_p^e$, as follows:

$$dv_p^e = \frac{\kappa}{1+e}\frac{dp}{p} , \tag{8}$$

$$(d\varepsilon_a)_p^e = 0 , \tag{9}$$

where $\kappa = 0.434\ Cs$.

4.3 Results of tests in which $dp > 0$ and $d\eta_a < 0$

Here we present results of tests carried out along stress paths where $dp > 0$ and $d\eta_a < 0$. Two kinds of experiments were conducted, which we will call series 1 and series 2 tests.

First we will describe the results of series 1 tests, in which each specimen was sheared to stress ratio η_{ai} while p was held constant, after being isotropically consolidated to the mean effective stress, p_i . Then, radial stress was increased and therefore stress ratio η_a was decreased while axial stress was kept constant. Each experiment was proceeded in steps, as indicated (by small circles) in Figure 9, separated by one day intervals. Initial stress values in these unloading tests correspond to those shown in Figure 2.

Figure 10 shows results of tests in which the value of η_{ai} was varied while p_i was kept constant (= 2 kgf/cm²). Figure 11 shows results of tests in which p_i was varied, while η_{ai} was held constant (= 0.75). In these figures, the stress-strain curves for the unloading tests in which p was held constant (Figures 3 and 4) are represented by solid lines. The initial unloading points of these curves coincides with those of the corresponding tests indicated by plots in this figure. Also in these figures, analytical curves to be described later are represented by dashed lines. In Figures 10(b) and 11(b), $\eta_a \sim v$ curves are quite similar to each other and independent of η_{ai} and p_i .

Next, we examine the results of series 2 tests. Figure 12 shows the stress paths used. Tests were

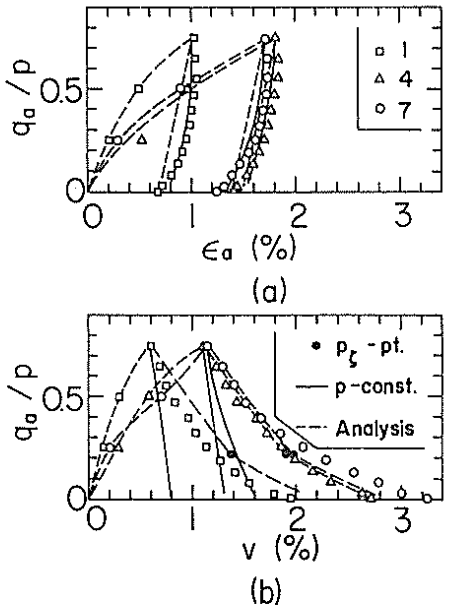

Figure 11 Comparison between experimental and analytical results of constant σ_a' tests (η_{ai} = 0.75)

performed in the same manner as in series 1. The stress conditions at initial unloading points for all tests were: p_i = 2 kgf/cm^2 and η_{ai} = 0.75.

In Figure 13 results of each test are plotted. The dashed lines are analytical curves (described below). It is apparent in Figure 13(a) that the $\eta_a \sim \varepsilon_a$ relationships for these tests are almost identical, irrespective of stress paths.

5 ANALYTICAL RESULTS

We have already shown that the $\eta_a \sim \varepsilon_a$ relationships during unloading are almost identical to the results of tests in which p was kept constant (Figures 10(a), 11(a) and 13(a)). Similar results have already been shown by Balasubramaniam (1975). Taking these facts into account, the following equation can be reasonably assumed in equation (4) when $|\eta_a|$ is decreased.

$$(d\varepsilon_a)_p^p = 0 \qquad (10)$$

Next we examine the volumetric behavior of soil specimens. Figures 14 and 15 show the relationship between $\{(-\delta e) - (-\delta e)_\eta\}$ and $(-\delta e)_p$, where $(-\delta e)_\eta$ represents a decrease in the void ratio from the initial unloading point of the corresponding constant p test, and $(-\delta e)_p$ also represents a decrease in the void ratio, calculated as follows:

$$(-\delta e)_p = \lambda \ln \frac{p}{p_i} \qquad (11)$$

In this calculation $\lambda \simeq 0.434$ Cc and Cc denotes the compression index. From Figure 7, we know Cc is equal to 0.244. In Figure 14 the data points which all lie clearly below the dashed line with a slope of one, have been approximated by two straight lines. Here we denote the value of $\{(-\delta e) - (-\delta e)_\eta\}$ at the point where the two lines intersect by Δe_0. Figure 16 shows this relationship schematically in an e_p $\{= e - (-\delta e)_\eta\} \sim \ln p$ plane. It is clear from this figure that when η_a is decreased and p is simultaneously increased, after the specimen is sheared under constant p ($= p_i$), the void ratio e_p is decreased by Δe_0 along a line of slope ζ ($< \lambda$), and then along a line which has a slope equal to λ. This phenomenon is a sort of p_c-effect, resulting from a sudden change of stress paths.

For the portion of the line where $\{(-\delta e) - (-\delta e)_\eta\} < \Delta e_0$ we denote the slope by i, and obtain the relationship, $\zeta = i \cdot \lambda$. If p_ζ denotes the value of p at the point where the two ζ lines in Figure 16

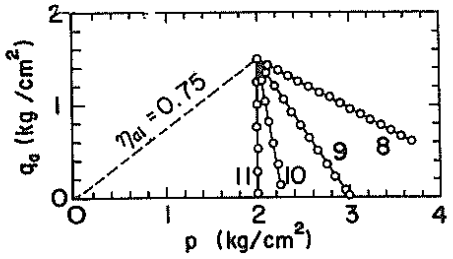

Figure 12 Stress paths of the unloading tests of series 2

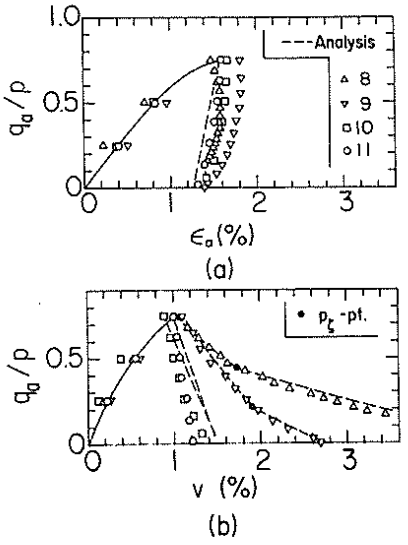

Figure 13 Comparison between experimental and analytical results (series 2)

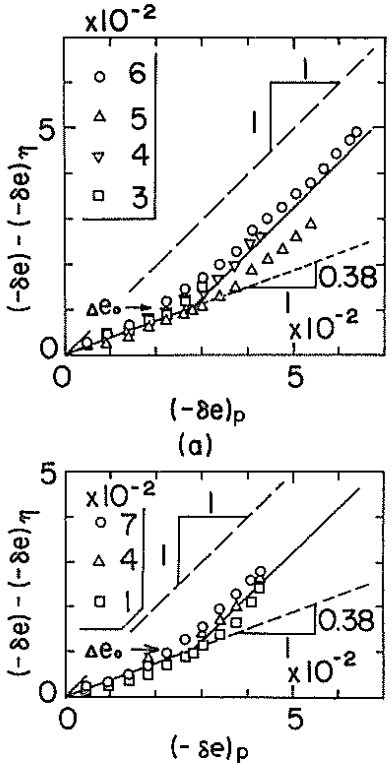

Figure 14 $\{(-\delta e) - (-\delta e)_\eta\} \sim (-\delta e)_p$ plots (series 1)

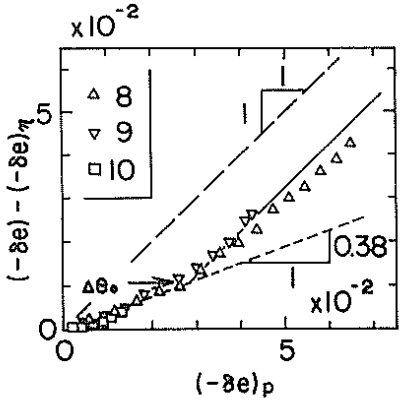

Figure 15 $\{(-\delta e) - (-\delta e)_\eta\} \sim (-\delta e)_p$ plots (series 2)

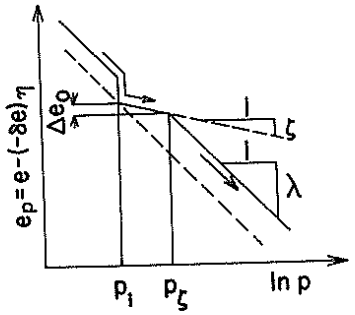

Figure 16 A relation between e_p and ln p

intersect, we obtain the following equation.

$$\Delta e_0 = \zeta \ln \frac{p_\zeta}{p_i} \qquad (12)$$

It is reasonable to assume from equation (12) that p_ζ/p_i is constant since it is clear in Figures 14 and 15 that Δe_0 and i are almost constant, irrespective of p_i and η_{ai} . Thus, when $(-\delta e)_p \leq \Delta e_0$,

$$dv_p^p = \frac{\zeta - \kappa}{1 + e} \frac{dp}{p} , \qquad (13)$$

and when $(-\delta e)_p > \Delta e_0$, dv_p^p can be expressed as:

$$dv_p^p = \frac{\lambda - \kappa}{1 + e} \frac{dp}{p} , \qquad (14)$$

From Figures 14 and 15, we obtain the following.

$$\Delta e_0 = 0.0106, \quad p_\zeta/p_i = 1.31, \quad \zeta = 0.040$$

In Figure 9 the constant, $p = p_\zeta = 1.31\, p_i$, is expressed by the dashed line. It is clear in this figure that most or all of the unloading process does not reach p_ζ when η_{ai} is small. As a result, the following relationships are obtained from tests with stress paths treated in this paper ($dp \geq 0$, $d\eta_a \leq 0$).

$$d\varepsilon_a = (d\varepsilon_a)_\eta^e = \frac{G}{M} d\eta_a \qquad (15)$$

$$dv = \frac{d}{M} |d\eta_a| + \frac{\zeta \text{ (or } \lambda)}{1 + e} \frac{dp}{p} \qquad (16)$$

Analytical results represented by the dashed curves in Figure 10, 11 and 13 were calculated using equations (15) and (16). Values of parameters used in these calculations are shown in Table 1. In Figures 10, 11 and 13, points corresponding to the points of intersection of the two lines in Figure 16 are shown as p_ζ points. Reasonable agreement was obtained between experimental and analytical results.

6 CONCLUSIONS

In this paper the elastic strain of soil is assumed to consist of two components, one caused by changes in stress ratio and the other by changes in mean effective stress. These components of elastic strain were studied by conducting by triaxial drained tests with various stress paths. From these tests the following conclusions were reached.

1) From the loading-unloading-reloading tests in which the stress ratio was varied while the mean effective stress was kept constant, $\eta_a/M \sim \varepsilon_a$ curve has the same slope during unloading as during reloading. The slope of the $\eta_a/M \sim \varepsilon_a$ curve under triaxial compression is almost equal to that of the same curve under triaxial extension. On the other hand, for volumetric strain, we observed irreversible behavior.

Table 1
Values of parameters used in the analysis

λ	0.106	Δe_0	0.0106
Mc	1.50	d	0.0067
ζ	0.040	G	0.0065

2) During unloading and reloading of p with η_a kept constant, e ~ log p curves exhibited nearly the same slope irrespective of η_a . Changes in deviatoric strain during swelling, while η_a is kept constant, are negligible. However, in reloading, the distortional strain increases gradually as p increases.

3) When the stress ratio is decreased and the mean effective stress is increased, the soil specimen shows the so-called p_c-effect in the relationship between e_p $\{= e - (-\delta e)_\eta\}$ and ln p. In these tests the $\eta_a \sim \varepsilon_a$ curves did not appear to be influenced by the effective stress paths.

7 ACKNOWLEDGMENT

The research described in this paper was carried out under supervision of Prof. T. Shibata of Kyoto University. Experimental work was carried out by Technical Official H. Shimizu under the author's supervision in Kyoto University. The author expresses his sincere acknowledgment to them.

8 REFERENCES

Balasubramaniam, A.S. (1975). Stress-strain behaviour of a saturated clay for state below the state boundary surface. Soils and Foundations, Vol. 15, No. 3, pp 13-26.

Karube, D. and Kurihara, N. (1966). On the dilatancy and shear strength of remoulded clay. Proc. JSCE, No. 135, pp 10-24.

Nishi,K. and Esashi, Y. (1978). Stress-strain relationships of sand based on elastoplasticity theory. Proc. JSCE, No. 280, pp 111-122.

Ohmaki, S. (1979). A mechanical model for the stress-strain behaviour of normally consolidated cohesive soil. Soils and Foundations, Vol. 19, No. 3, pp 29-44.

Poorooshasb, H.B., Holubec, I. and Sherbourne, A.N. (1966). Yielding and flow of sand in triaxial compression, Part 1. Can. Geotech. Journ., Vol. 3, No. 4, pp 179-190.

Tatsuoka, F. and Ishihara, K. (1974). Yielding of sand in triaxial compression. Soils and Foundations, Vol. 14, No. 2, pp 63-76.

Vermeer, P.A. (1978). A double hardening model for sand. Geotech., Vol. 28, pp 413-433.